Published in final edited form as:

Bone. 2020 August ; 137: 115364. doi:10.1016/j.bone.2020.115364.

Juvenile Paget's Disease From Heterozygous Mutation of *SP7* Encoding Osterix (Specificity Protein 7, Transcription Factor Sp7)

Michael P. Whyte[1,2], **Philippe M. Campeau**[3], **William H. McAlister**[4], **G. David Roodman**[5], **Nori Kurihara**[5], **Angela Nenninger**[1], **Shenghui Duan**[2], **Gary S. Gottesman**[1], **Vinieth N. Bijanki**[1], **Homer Sedighi**[6], **Deborah J. Veis**[1,2], **Steven Mumm**[1,2]

[1]Center For Metabolic Bone Disease and Molecular Research, Shriners Hospitals for Children – St. Louis; St. Louis, MO 63110, USA

[2]Division of Bone and Mineral Diseases, Department of Internal Medicine, Washington University School of Medicine; St. Louis, MO 63110, USA

[3]Department of Pediatrics, University of Montreal; Montreal, Quebec H3T 1C5, Canada

[4]Mallinckrodt Institute of Radiology, Washington University School of Medicine at St. Louis Children's Hospital; St. Louis, MO 63110, USA

[5]Indiana University School of Medicine; Indianapolis, IN 46202, USA

[6]Department of Plastic Surgery, Washington University School of Medicine at St. Louis Children's Hospital; St. Louis, MO 63110, USA

Abstract

Juvenile Paget's disease (JPD) became in 1974 the commonly used name for ultra-rare heritable occurrences of rapid bone remodeling throughout of the skeleton that present in infancy or early childhood as fractures and deformity hallmarked biochemically by marked elevation of serum alkaline phosphatase (ALP) activity (hyperphosphat*asemia*). Untreated, JPD can kill during childhood or young adult life. In 2002, we reported that homozygous deletion of the gene called tumor necrosis factor receptor superfamily, member 11B (*TNFRSF11B*) encoding osteoprotegerin (OPG) explained JPD in Navajos. Soon after, other bi-allelic loss-of-function *TNFRSF11B* defects were identified in JPD worldwide. OPG inhibits osteoclastogenesis and osteoclast activity by decoying receptor activator of nuclear factor κ-B (RANK) ligand (RANKL) away from its receptor RANK. Then, in 2014, we reported JPD in a Bolivian girl caused by a heterozygous activating duplication within *TNFRSF11A* encoding RANK. Herein, we identify mutation of a third gene underlying JPD. An infant girl began atraumatic fracturing of her lower extremity long-

Correspondence To: Michael P. Whyte, M.D., Shriners Hospitals for Children-St. Louis, 4400 Clayton Avenue, St. Louis, MO 63110, USA, Telephone: 314-872-8305, mwhyte@shrinenet.org.

Author Contributions: All authors helped write and approved the submitted manuscript. MPW was referred and examined the patient, organized the clinical and research studies, and drafted and finalized the manuscript. PMC interpreted the whole exome sequence data. WHM delineated the skeletal radiographic findings. GDR with NK excluded presence of measles virus transcripts. AN assisted with the chart review. GSG and VB helped illustrate the manuscript. HS characterized the dental findings. SM organized the exome sequencing and with SD verified the sporadic *SP7* missense mutation.

Disclosures: None.

bones. Skull deformity and mild hearing loss followed. Our single investigation of the patient, when she was 15 years-of-age, showed generalized osteosclerosis and hyperostosis. DXA revealed a Z-score of +5.1 at her lumbar spine and T-score of +3.3 at her non-dominant wrist. Biochemical studies were consistent with positive mineral balance and several markers of bone turnover were elevated and included striking hyperphosphatasemia. Iliac crest histopathology was consistent with rapid skeletal remodeling. Measles virus transcripts, common in classic Paget's disease of bone, were not detected in circulating mononuclear cells. Then, reportedly, she responded to several months of alendronate therapy with less skeletal pain and correction of hyperphosphatasemia but had been lost to our follow-up. After we detected no defect in *TNFRSF11A* or *B*, trio exome sequencing revealed a *de novo* heterozygous missense mutation (c.926C>G; p.S309W) within *SP7* encoding the osteoblast transcription factor osterix (specificity protein 7, transcription factor Sp7). Thus, mutation of *SP7* represents a third genetic cause of JPD.

Keywords

Alkaline Phosphatase; Bone Remodeling; Dental Pathology; Dento-osseous Disease; Fractures; Hyperostosis; Hyperphosphatasemia; Measles Virus; Osteoblast; Osteoclast; Osteoprotegerin; Osteosclerosis; Osterix; Paget Bone Disease; Woven Bone

II) Introduction:

In 1956, Harry Bakwin, MD and Marvin S. Eiger, MD[(1)] reported from Bellevue Hospital in New York City, USA, a 7-year-old Puerto Rican girl with fragile and deformed long-bones, macrocranium, and elevated serum alkaline phosphatase (ALP) activity (hyperphosphat*asemia*). Her skeletal histopathology indicated rapid bone remodeling not considered a form of osteogenesis imperfecta or Paget's disease of bone (PDB). Their publication is the first descripton of what in 1974 came to be commonly called juvenile Paget's disease (JPD).[(2)] In the interim, the disorder had been given nearly as many names as there were case reports (OMIM #239000).[(3)] Early on, JPD was correctly viewed as an autosomal recessive (AR) entity[(3)] and considered a skeletal dysplasia[(4)] that presents in infancy or early childhood with bone fragility, deformity, and pain followed by conductive hearing loss.[(5–7)] Until bone antiresorptive pharmaceuticals became available, JPD was often fatal by young adult life.[(5,8)] If survival was longer, generalized arterial calcification resembling this complication in pseudoxanthoma elasticum[(8,9)] frequently led to retinopathy with blindness,[(10)] and perhaps also explained rare cerebral artery aneurysms.[(11)] Some patients with a variant of JPD had relatively mild skeletal disease but with significant mental retardation.[(12)] However, only ~ 80 instances of JPD have been reported.[(3,5,13)]

In 2002, we found[(5)] in two Navajos from the southwest United States the first explanation for JPD; i.e., homozygous selective and complete deletion of the gene *TNFRSF11B* (OMIM *602643)[(3)] that encodes tumor necrosis factor receptor superfamily, member 11B that is commonly called osteoprotegerin (OPG).[(3)] OPG is the decoy molecule for receptor activator of nuclear factor-κB (RANK) ligand (RANKL) (OMIM *602642)[(3)] that is sometimes called osteoclast (OC) differentiation factor. RANKL, when it binds to RANK (OMIM *603499),[(3)] promotes bone resorption by enhancing OC formation from

hematopoietic progenitor cells as well as by activating mature OCs.[14–17] Therefore, OPG suppresses skeletal turnover. Navajos with JPD have in their circulation no detectable OPG and markedly elevated soluble RANKL.[5] Soon after our report, most but not all JPD patients worldwide were found to carry distinctive homozygous loss-of-function defects in *TNFRSF11B* representing geographic "founder" mutations.[5,6,18–21] Then, in 2014, we discovered in a 13-year-old Bolivian girl the second genetic basis for JPD, a unique heterozygous in-frame activating 15-bp tandem duplication within exon 1 of *TNFRSF11A* that encodes the signal peptide of RANK.[22]

Herein, we report the third gene that can underlie JPD. We identify in a teenage girl a heterozygous missense mutation (c.926C>G; p.S309W) within *SP7* (OMIM: *606633)[3] that encodes the osteoblast (OB) transcription factor specificity protein 7 or transcription factor SP7, commonly called osterix (OSX).

III) Materials and Methods:

The patient was referred to us at age 15 years in 2000 and then admitted once to the Center for Metabolic Bone Disease and Molecular Research, Shriners Hospitals for Children – St. Louis, St. Louis, MO, USA. The father and a physician friend accompanied her. Informed written consent was obtained from the patient and her parents as approved by the Institutional Review Board, Washington University School of Medicine, St. Louis, MO, USA (WUSM). Two years later, when we reported OPG deficiency in Navajo patients as the first genetic cause of JPD,[5] we mentioned that despite her JPD she had shown no mutation of *TNFRSF11B*.

A) Medical History:

The patient weighed 3.5 kgs (7.7 lbs) at nearly full-term birth and had neonatal jaundice. Breast feeding continued until 7 months-of-age. It was uncertain if vitamins were given.

She seemed well until 8 months-of-age when her right tibia fractured as she was being dressed with stockings. Healing occurred on time, but leg deformity became apparent. Then, a stress fracture in the anterior tibial cortex was treated by osteotomy.

At about 3 years-of-age, her right femur broke from a fall and healed with casting, but leaving additional deformity. Several months later, her left tibia fractured and was treated using orthopedic metal. PDB was considered her diagnosis. Subsequently, another tibial fracture required a longer medullary rod. Then, a femur fracture became infected necessitating orthopedic metal removal. Despite a six-week course of antibiotics, osteomyelitis recurred, including an open wound. After further treatment, angular deformity of the left femur was corrected surgically.

By 11 years-of-age, 20 fractures were counted. During the next two years, injections of salmon and human calcitonin reportedly failed to diminish her hyperphosphatasemia. Vomiting and sometimes paresthesias and carpal spasm could follow the injections. Calcium supplements were begun prophylactically. Calcitonin therapy ended at age 13 years, but we

did not learn if it was helpful. Menarche occurred at age 12 years with regular menses thereafter.

At age 14 years, her frontal bones became prominent with bony protuberances of her left face. Swelling of her cheeks and eyes with fever up to 40°C lasted one week. Antibiotics seemed effective, including for several recurrences.

During the year before referral to us, no fractures or facial swellings had occurred, her forehead prominence had diminished, and there had been no hospitalizations, surgeries, or other diagnoses. High-tone hearing loss was noted. Eyeglasses had been prescribed two years previously. Scoliosis with six centimeter shortening of her left lower extremity was identified but no shoe lift was worn. Bilateral femoral and tibial intramedullary rodding was in place. Pain in her left thigh perhaps reflected an old fracture, and pretibial discomfort was attributed to “rheumatism” because she had worn wet plaster casts. Low back pain accompanied weather changes. Intermittent mild headaches were worse during viral illnesses when her eyes and cheeks would swell. Osteomyelitis had not recurred for five years. She had never fractured her upper limbs.

Review-of-systems revealed no dizziness, diplopia, or urinary tract symptoms. Her family history was negative for consanguinity or skeletal abnormalities. Her 7-year-old brother, father and his three siblings, and mother and her five siblings were all reportedly well.

To prepare for an iliac crest biopsy, the patient received oxytetracycline 250 mg po thrice daily for three-days, but a course of tetracycline hydrochloride became necessary when an amoebic stool infection was documented.

B) Physical Examination:

Vital signs were temperature 36.7°C, pulse 80, respirations 24, and blood pressure 100/64. Height was 170 cm (5 ft, 7 in) (Z-score +1.3), weight 58 kg (128 lbs) (Z-score +0.6), arm span 180 cm, sitting height 91 cm, and head circumference 53 cm [~ 25th centile, excluding macrocranium but with a narrow vertex (acrocephaly)]. Cranial nerve and neurovascular examinations were intact. Her fontanelles were closed and hypertelorism was evident while her palpebral fissures seemed small *vis-a-vis* her broad forehead (Figure 1 a–c). Extraocular muscle movements were intact. No tenderness occurred from pressing her facial bones. Clinical and radiographic dental examination revealed a number of abnormalities (see Dental Findings). Skeletal deformity caused her to limp and consisted primarily of anterior bowing of her right lower limb, considerably shorter left lower limb, and scoliosis (Figure 1 d–f).

Her skin was unremarkable. The upper extremities showed no cyanosis, clubbing, deformity, or tenderness when gently squeezed. No pain occurred upon compressing her ribs or pushing on her scapulae or clavicles. Marked kyphosis deformed her thoracolumbar junction, and there was a left lumbar hump. No spinal tenderness occurred from gentle fist percussion. No hepatosplenomegaly, abdominal mass, or costovertebral angle tenderness was detected. Multiple scars on her extremities reflected ten previous orthopedic procedures. The hips had good internal and external rotation, and she could readily straight leg raise to > 90°. Passive

flexion/extension of her knees was without crepitus, and there was no tenderness from gentle thumping or squeezing of her femora or feet. Varus deviation of the right foot was apparent.

C) Biochemical Studies:

We matched, based on a 7-day food record, her typical dietary calcium intake (~ 400 mg daily) during her admission. Fasting blood and a 24-hour urine collection provided routine and research specimens for studies of mineral homeostasis performed in our CLIA-certified laboratory.[23,24] Serum multiplex biomarker profiling[25–27] was not yet available to us.

D) Radiological Studies:

We reviewed our patient's six referral radiographs and then obtained a skeletal survey and bilateral long-leg cassette imaging, whole-body technetium-99m bone scintigraphy, and dual-energy x-ray absorptiometry (DXA) (Hologic 4500-A, Waltham, MA, USA).

E) Histological Studies:

Left iliac crest trephine biopsy specimens were placed into Millonig's fixative for non-decalcified histopathology and into gluteraldehyde for electron microscopy.

F) Mutation Analysis:

The aforementioned informed written consent included genetic testing to discover the etiology of the patient's skeletal disease. Peripheral blood leukocyte DNA was obtained from her and her parents using the Puregene DNA Extraction Kit (Gentra Systems, Minneapolis, MN, USA). Beginning in 2002, and then over the next decade as they emerged in the literature, the following candidate genes were assessed by Sanger-sequencing including all coding exons and adjacent mRNA exon/intron splice sites: *TNFRSF11B* encoding OPG (2002), *TNFRSF11A* encoding RANK (2004), *SQSTM1* encoding sequestosome (2006), *TNFSF11* encoding RANKL (2008), *sFRP1* encoding secreted frizzled related protein 1 (2009), and *TNFSF10* encoding TNF-related apoptosis-inducing ligand (TRAIL) (2011). Primer sequences and conditions are available from us on request. Then, with negative results thus far, trio-exome sequencing and analysis was carried out in 2012 at the Genome Technology Access Center, WUSM. Anticipating an autosomal recessive form of JPD, 21 genes showing compound heterozygous variants were identified, but not studied further as they were deemed unrelated to bone biology. However, in 2016, trio exome sequence analysis was again performed, now at the University of Montreal, Montreal, Quebec, Canada. Data processing, alignment (using a Burrows-Wheeler algorithm, BWA-mem v0.7.5a), variant calling, and annotation were carried out with the Genome Analysis Toolkit (GATK) UnifiedGenotyper v2.6–4 tool (https://www.broadinstitute.org/gatk/guide/tooldocs/org_broadinstitute_gatk_tools_walkers_genotyper_UnifiedGenotyper.php). Variant annotation used an in-house pipeline and Annovar v2014–11-12 (http://www.openbioinformatics.org/annovar/). Human and mouse phenotypes for each gene were annotated using Orphanet (https://www.orpha.net/consor/cgi-bin/index.php) and OMIM[3] (https://www.omim.org/), and the protein function using Uniprot (https://www.uniprot.org/).

Confirmatory Sanger sequencing of the patient's altered and parents' unaltered *SP7* gene was then performed in 2016 at our research laboratory at WUSM.

G) Measles Virus Transcript Analysis:

Measles virus nucleocapsid protein (MVNP) mRNA expression was determined byqRT-PCR using total RNA isolated from mononuclear cells in a whole blood sample.[28] The gene-specific primers for MVNP were 5′-AGTTCCACATTAGCATCTGAAC-30 (sense) and 5′-TACTGATCTTGTCCTCAGTAG-30 (antisense) (GenBank accession number M10297X01999).

IV) Results:

A) Mutation Analysis:

Candidate gene Sanger-sequencing was negative for *TNFRSF11B* encoding OPG, *TNFRSF11A* encoding RANK, *SQSTM1* encoding sequestosome, *TNFSF11* encoding RANKL, *sFRP1* encoding secreted frizzled related protein 1, and *TNFSF10* encoding TNF-related apoptosis-inducing ligand (TRAIL). Trio-exome sequencing undertaken between 2012–2016 revealed in the patient: i) homozygous rare variants in *AP4B1, POLR1A, ANKRD36, RGPD4, RGPD5, RGPD8, RANBP2, RRP1B, PCNT,* and *NOTCH4*; ii) one set of compound heterozygous variants in *MUC5B*; and iii) five *de novo* heterozygous variants in *USP17L13, ACHE, MPG, CDC27*, and *SP7*. Soon after, our Sanger-sequencing confirmed that her heterozygous missense variant in *SP7* (NM_152860.1: c.926C>G, p.Ser309Trp) was absent in her parents and from the Exome Aggregation Consortium (ExAC) browser (http://exac.broadinstitute.org). The etiology of our patient's skeletal disorder therefore seemed consistent with the *de novo SP7* variant (p.Ser309Trp) based on the known role of the gene's product OSX as a transcription factor in OB development and that bi-allelic *SP7* loss-of-function causes osteogenesis imperfecta type XII.[3,29] Her mutation was predicted by both SIFT and PolyPhen2 to be damaging as it would affect a highly conserved residue in the first zinc finger domain.[30,31] OSX has an amino-terminal transactivation domain and a carboxy-terminal DNA-binding domain comprising three zinc finger motifs.[32] Ser 309, changed in our patient, is located in the center of the first zinc finger domain and is separated by two and three amino acid residues from two acetylated lysine residues (Lys 307 and Lys 312, respectively). In 2016, Lu et al[33] reported that this site-specific acetylation enhanced SP7 stability, DNA binding ability, and transcriptional activity. Hence, our patient's mutation, Ser309Trp, likely affected these functions. Supporting the pathogenicity and consequent phenotype of this *SP7* mutation, we found the 2019 preliminary report from Lui et al[34] of a boy with cranial hyperostosis, long bone fragility, and increased numbers of OBs carrying this identical *SP7* defect (p.Ser309Trp).

B) Biochemical Findings:

Routine investigation of our patient's mineral metabolism (Table 1) was normal except for mild elevation of serum intact parathyroid hormone (PTH) together with low urinary calcium (Ca) excretion, perhaps reflecting her low dietary Ca intake as well as positive mineral balance indicated by the radiographic and DXA studies (see Radiological Findings). Mild anemia and reduction of serum IGF1 were not explored.

Serum ALP activity and urinary total hydroxyproline (Quest Diagnostics, Inc.; San Juan, Capistrano, CA, USA) were both markedly elevated in keeping with accelerated bone turnover, yet urinary deoxypyridinoline was inexplicably normal. Bone-specific ALP was not assayed. In 2002, we had reported that her serum RANKL and OPG levels were normal.[5] Serum acid phosphatase and creatine kinase, that can be elevated in osteopetroses,[24] were normal as was lactate dehydrogenase that is often increased in Albers-Schönberg autosomal dominant osteopetrosis.[23]

C) Radiological Findings:

As detailed below, the patient's referral radiographs and then radiological studies at age 15 years were especially notable for generalized trabecular bone coarsening (osteosclerosis) and cortical bone thickening (hyperostosis) and foci of increased radio-isotope uptake on skeletal scintigraphy. Together the findings were consistent with a relatively mild form of JPD (see Discussion).

1) Referral Radiographs: Among the six referral radiographs (Figure 3), the earliest at age two years showed apex lateral bowing of the distal right tibia together with mild anterior bowing. The bones were sclerotic with cortical thickening. At age 3 years, the right femur had a transverse pathologic fracture apex lateral, marked osteosclerosis, and lucent striated lines distally including the epiphysis. Proximally, the medullary cavity was obliterated. At an older age, another transverse fracture had occurred more distally in the right femur that manifested lateral bowing, a markedly thickened cortex, osteopenia distally, and small longitudinal lucent lines and small cystic areas in the sclerosis throughout the thickened cortex. Later, the right femur and tibia/fibula showed obliteration of the medullary cavities where the sclerotic bone had longitudinal small lucent channels and cystic areas as well as transverse stress fractures.

2) Radiographic Skeletal Survey: The radiographic skeletal survey at age 15 years (Figure 4) showed the skull's diploic space was markedly thickened and sclerotic and contained small lucencies throughout. The base, maxilla, and petrous bones also were markedly osteosclerotic. Sinus development was apparent, but the frontal sinuses contained osteosclerotic filling defects. The maxillary sinuses were small. There were frontal digital markings and marked hypertelorism. In the sclerotic petrous bones, the semicircular canals and cochlea were apparent. The sella turcica was small. Only portions of the lambdoid suture and coronal sutures were seen. The mental process was large. The mandible was diffusely osteosclerotic with cortical thickening. The teeth were markedly deformed with hypoplastic roots (see Dental Findings).

A humerus showed sclerosis with marked cortical thickening encroaching on the medullary cavity and obliterating it proximally. Linear lucencies and coarse trabeculae were present distally. The right radius head was dislocated and deformed, and did not articulate with the humerus. Bowing deformities of both forearm bones accompanied diffuse osteosclerosis, obliteration of the medullary cavities, and linear and small lucencies scatted throughout. The hands demonstrated some lack of modeling in the distal radius and ulna, diffuse osteosclerosis, and marked coarse linearly-arranged thick trabeculae. Patchy sclerosis was

apparent in the middle and distal phalanges. The carpal bones were almost uniformly sclerotic with small lucencies. The ribs were markedly sclerotic and expanded throughout with thick trabeculae and small longitudinal lucencies. The clavicles were thickened, sclerotic, and expanded. Vertebrae were markedly sclerotic. Scoliosis was greatest in the lumbar region where vertebral bodies had an anterior indentation resembling an hourglass. The pelvis was asymmetric associated with left lower extremity shortening, diffuse and marked osteosclerosis, and contained small lucencies and thick trabeculae. Coxa valga was present on the right where femoral plate and screws were in place, and coxa vara on the left was associated with an intramedullary rod. The lower extremities showed shortening on the left, marked osteosclerosis, cortical thickening, and coarse linear striations primarily in the metaphyses. The femora were deformed with a pseudofracture extending on the medial side below the lesser trochanter on the right. The right tibia was bowed with partial surgical removal of the mid-right fibula. Medullary cavities were obliterated except for the metaphyses of the distal femora and tibii. Both feet had heel and forefoot varus with generalized osteosclerosis with prominent linear lucencies scattered throughout. Linear coarse striata-appearing trabeculae were especially apparent in the metaphyses, but also in the tarsal bones including the calcaneus. Incomplete fractures of the metatarsals were present bilaterally.

3) Skeletal Scintigraphy: Delayed whole-body bone scintigraphy using Tc-99m diphosphonate demonstrated irregular uptake in all bones (Figure 5).

4) Dual-Energy X-ray Absorptiometry: DXA of the patient's scoliotic L_1-L_4 spine showed areal BMD of 1.546 gm/cm^2 (Z-score = +5.1; 156% for age and sex) and bone mineral content (BMC) of 112 gms. Her left wrist total BMD was 0.727 gm/cm^2 (T-score = +3.3; control data not available for age- and sex). Hip assessment was obviated by orthopedic metal.

D) Iliac Crest Histopathology:

Undecalcified iliac crest sections prepared at the Armed Forces Institute of Pathology (AFIP), Washington, DC, USA in 2000 revealed histopathological findings consistent with JPD, although routine histomorphometry was precluded because the specimen consisted almost entirely of cortical bone. The Haversian systems had thick osteoid seams, and showed evidence of excessive bone resorption as they were widened with active OC activity. Polarized-light microscopy reportedly showed ~ 50% of the matrix was woven bone. However, closure of the AFIP in 2011 precluded access to the blocks or slides to illustrate these findings or to learn the results of the electron microscopy. Nevertheless, we were able to obtain from the AFIP some photographs of the histopathology (Figure 6).

E) Dental Findings:

The patient's extra-oral examination was within normal limits. No temporomandibular joint disorder was reported or detected, including no clicking. No shifting or deviation of the mandible occurred during opening or closing, and its lateral movements were normal. No significant clinical soft tissue pathology was detected. Oral hygiene was fair. Class II permanent molar occlusion was detected. The midline relationship of the maxilla and

mandible was good. Overjet was 2 mm, and overbite 80%. Consequently, she had a deep bite. No crowding of the dentition or posterior cross-bite was found. The following permanent teeth were present: #3, 4 (90° rotated), 5 (45° rotated) − 11, 14, 19, 21 (partially erupted and 90° rotated), #22 – 28, and 30. The following deciduous teeth were present: #I (root tips), #J (had pulpotomy), #K, and #T (root tips). Dental treatment was necessary for teeth #3, 14, 21, 30 with occlusal carious lesions needing restoration. Teeth #J, K, T, and 19 were badly broken down, and needed extraction.

Eight periapical dental radiographs indicated the erupted permanent teeth had blunted (rounded) apices, short roots (at best half-normal length), some with very thin pulp canals or no pulp canal or chamber yet not affecting the clinical crown color, some with enlarged periodontal ligaments, some having alveolar bone resorption predisposing to deep periodontal pockets and gingival recession, tooth #21with an apical radiolucency, and teeth #13, 20, 29, and 31 showing bony impaction and needing extraction (Figure 7).

F) Measles Virus Studies:

We found no evidence of measles virus nucleocapsid protein mRNA expression in the patient's whole blood mononuclear cells.

G) Clinical Course:

In keeping with PDB treatment circa 2000,[35] a six-month course of alendronate (40 mg po daily) was prescribed. A multivitamin with iron and better dietary Ca intake were also recommended. To assess her response, baseline and follow-up retinal examination, audiometry, and biochemical studies of bone and mineral homeostasis were advised. Correspondence from her father eight months later reported her serum ALP had corrected to 282 U/L (age-matched Nl, < 296).

V) Discussion:

Juvenile Paget's disease (JPD) was assigned, since 1956 when first described,[1] many names including *hyperostosis corticalis deformans juvenilis* and hereditary hyperphosphatasia (OMIM #239000).[3] Case reports during the subsequent two decades seemingly all designated the disorder differently. Nevertheless, its presentation in infancy or early childhood with bone pain, debilitating fractures, deformities, and growth retardation has always been understood to reflect markedly accelerated skeletal remodeling featuring excess weak and disorganized woven bone.[12,35,36] Hence, in 1974,[2] the eponym JPD became commonly used.[7,37] From its initial description,[1] however, JPD was appreciated not to be a severe form of PDB (OMIM #167250),[3] which features monostatic or polyostotic accelerated bone turnover typically occurring sporadically and presenting in middle-age or later.[38–40] JPD manifests early in life the fastest bone turnover of any skeletal disease, and osteosarcoma has occurred.[7] In classic PDB, genetic predisposition has been identified for many patients[41] and paramyxoviridae infection, predominantly measles virus, is implicated in its pathogenesis.[40] In 2011, we reported that 70% of the patients with PDB we tested expressed MVNP transcripts in their marrow, whereas such transcripts were not detected in the nine normal donors.[28] Herein, MVNP transcripts were

not found in the circulating mononuclear cells of our patient who lacked the focal clinical and imaging characteristics of classic PDB.[38,40]

Identification of the RANKL/OPG/RANK/NF-κB signaling pathway as the principal regulator of OC formation and action began during 1997–1998 with the discovery of RANKL, its "decoy" receptor OPG, and its receptor RANK within the tumor necrosis factor (TNF) superfamily.[42] Genetically altered mice revealed that osteoclastogenesis is accelerated or slowed by binding of RANKL to RANK versus OPG, respectively.[43] In 1998, vascular calcification was recognized in OPG knockout mice, and therefore some considered calling OPG "osteovasculoprotegerin".[44] Soon after, in 2000,[45] germline gain-of-function duplications within *TNFRSF11A* (RANK) began to explain ultra-rare disorders that resemble classic PDB (OMIM #167250),[3] but instead manifest accelerated remodeling throughout the skeleton.[7] Predictably, in 2007 and 2008, AR loss-of-function mutations in *TNFSF11* encoding RANKL[46] and *TNFRSF11A* encoding RANK[47] were discovered to cause "OC poor" osteopetroses involving inactive skeletal resorption.[7]

From 2002 when Whyte et al,[5] and soon after Cundy et al[18] and then others, found bi-allelic loss-of-function mutations within *TNFRSF11B*, JPD could be called "OPG deficiency". The defects within *TNFRSF11B*, underlying what we now call JPD-1, differ worldwide[19] but typically represent "founder" mutations.[37] The OPG deficiency[7] leads during young adult life to diffuse arterial calcification[44] that likely explains the retinopathy with blindness[8–10] and perhaps carotid aneurysms.[11] We now designate the JPD caused by activation of RANK[22] JPD-2, and the still idiopathic JPD associated with mental retardation[12] JPD-3.[7] Because this nosology seems useful, our current patient harboring a mutation of *SP7* encoding OSX will henceforth represent JPD-4.

OSX, also called transcription factor Sp7 or specificity protein 7, is a member of the Sp family of zinc-finger transcription factors,[48] key for OB function[49] and differentiation,[33,50] and is present specifically in these cells. Osx binds transcription factors Dlx 3, 5, and 6 to function as a co-factor for osteogenic gene expression,[50] while some consider that it couples directly the promoters of such genes. Thus, OSX is a master regulator of bone formation during embryonic development and bone homeostasis in adults. It is highly conserved among bone-forming vertebrates,[51,52] and key along with *Runx2* and *Dlx5* for differentiating mesenchymal precursor cells into OBs and eventually osteocytes.[53] Osx also inhibits chondrocyte differentiation, thereby balancing mesenchymal precursor cell differentiation into bone or cartilage,[54] although we note our patient was 5 feet 7 inches tall. Genome-wide association studies (GWAS) have shown the *SP7* locus is strongly associated with bone density.[55] Additionally, *SP7*: i) has been implicated in osteogenesis imperfecta (OI),[29] ii) mutations are associated with bone abnormalities in vertebrates, and iii) a mouse embryo model featuring Sp7 expression knock out forms no bone tissue.[48] Two principal pathways induce Sp7/Osx gene expression, directly or indirectly: i) Msx2 can directly induce Sp7, whereas ii) BMP2 indirectly induces Sp7 through Dlx5 or Runx2.[53] When Sp7 expression is triggered, many OB genes necessary for ossified bone formation are induced including Col1a1, osteonectin, osteopontin, and bone sialoprotein.[51] Negative regulation involves p53, microRNAs, and the TNF inflammatory pathway.[53] Dysregulation of the TNF pathway that leads to a block in bone growth by OBs partially explains the

increased degradation of bone in osteoporosis and rheumatoid arthritis.[56] Accelerated healing follows implantation of Sp7-overexpressing bone marrow stromal cells at fracture sites by inducing neighboring cells to activate genes characteristic of bone progenitors.[57] In fact, Sp7 expression is lower in mouse and human osteosarcoma cell lines compared to OBs and correlates with metastatic potential. Transfection of *SP7* into mouse osteosarcoma has reduced malignancy *in vitro*, including tumor incidence and volume, lung metastasis, and bone destruction.[58]

Apparent activation of OSX is illustrated by our patient's genetic disorder. It uniquely shows that the generalized rapid bone turnover of JPD can result not only from increased osteoclastogenesis and OC action as in JPD-1 and −2, but also from missense mutation of *SP7* that instead seems to accelerate OB activity while retaining some "cross-talk" between these two functionally opposite skeletal cell types. Although JPD-4 fundamentally features excess OB activity, our patient understandably seems to have benefitted from antiresorptive bisphosphonate therapy.

Thus, we have identified a missense mutation within *SP7* encoding OSX as a third etiology for JPD; i.e., JPD-1 reflecting AR usually homozygous loss-of-function mutations within *TNFRSF11B* encoding OPG, JPD-2 reflecting a specific AD activating duplication within the signal peptide sequence of *TNFRSF11A* encoding RANK, and JPD-4 reflecting a specific AD apparently activating missense mutation within *SP7* encoding OSX. A genetic basis for JPD-3 featuring mental retardation and other enigmatic instances of the JPD phenotype (unpublished) remains presumptive, but now discoverable using next generation sequencing.[59]

Acknowledgements:

Our report was made possible by the skill and dedication of the nursing, laboratory, and dietary staff at the Center for Metabolic Bone Disease and Molecular Research, Shriners Hospitals for Children - St. Louis, St. Louis, MO, USA. We thank William M. Cohen, DMD, MS for reviewing our patient's dental radiographs, and Ms. Margaret Huskey for mutation analysis. Mary P. Rosman, MD, DO kindly referred the patient. Ms. Sharon McKenzie provided expert secretarial help.

Funded In Part By: Shriners Hospitals for Children, The Clark and Mildred Cox Inherited Metabolic Bone Disease Research Fund at The Barnes-Jewish Hospital Foundation, Fonds de Recherche du Québec-Santé, and the Canadian Institutes of Health Research

VII) References:

1. Bakwin H, Eiger MS. Fragile bones and macrocranium. J Pediatr 49:558–564, 1956 [PubMed: 13368018]
2. Doyle FH, Woodhouse NJ, Glen AC, Joplin GF, MacIntyre I. Healing of the bones in juvenile Paget's disease treated by human calcitonin. Br J Radiol 47:9–15, 1974 [PubMed: 4809438]
3. Online Mendelian Inheritance in Man OMIM. Available at http://www.ncbi.nlm.nih.gov/entrez/dispomim.cgi?id_239000. Accessed December 19, 2019
4. Spranger Jürgen W., Brill Paula W., Poznanski Andrew (eds), "Bone Dysplasias: An Atlas of Genetic Disorders of Skeletal Development", 2nd Ed. Oxford University Press, Oxford, UK. pp: 509–10, 2002
5. Whyte MP, Obrecht SE, Finnegan PM, Jones JL, Podgornik MN, McAlister WH, Mumm S. Osteoprotegerin deficiency and juvenile Paget's disease. N Engl J Med 347:175–184, 2002 [PubMed: 12124406]

6. Whyte MP. Paget's disease of bone and genetic disorders of RANKL/OPG/RANK/ NF-κB signaling. Ann N Y Acad Sci 1068:143–164, 2006 [PubMed: 16831914]
7. Whyte MP. Mendelian disorders of RANKL/OPG/RANK/NF-κB signaling, Chapter #26 In: "Genetics of Bone Biology and Skeletal Disease" (2nd Ed) Thakker RV, Whyte MP, Eisman J, Igarashi T (eds) Elsevier (Academic Press), San Diego, CA, pp 453–68, 2018.
8. Mitsudo SM. Chronic idiopathic hyperphosphatasia associated with pseudoxanthoma elasticum. J Bone Joint Surg Am 53:303–314, 1971 [PubMed: 4926047]
9. Fretzin DF. Pseudoxanthoma elasticum in hyperphosphatasia. Arch Dermatol 111:271–272, 1975 [PubMed: 163620]
10. Sharif KW, Doig WM, Kinsella FP. Visual impairment in a case of juvenile Paget's disease with pseudoxanthoma elasticum: An eleven year follow up. J Pediatr Ophthalmol Strabismus 26:299–302, 1989 [PubMed: 2621550]
11. Allen CA, Hart BL, Taylor CL, Clericuzio CL. Bilateral cavernous internal carotid aneurysms in a child with juvenile Paget disease and osteoprotegerin deficiency. Am J Neuroradiol 29:7–8, 2008 [PubMed: 17947367]
12. Golob DS, McAlister WH, Mills BG, Fedde KN, Reinus WR, Teitelbaum SL, Beeki S, Whyte MP. Juvenile Paget disease: lifelong features of a mildly affected young woman. J Bone Miner Res 11:132–42, 1996 [PubMed: 8770706]
13. Chong B, Hegde M, Fawkner M, Simonet S, Cassinelli H, Coker M, Kanis J, Seidel J, Tau C, Tuysuz B, Yuksel B, Love D, Cundy T, The International Hyperphosphatasia Collaborative Group Idiopathic hyperphosphatasia and TNFRSF11B mutations: Relationships between phenotype and genotype. J Bone Miner Res 18:2095–2104, 2003 [PubMed: 14672344]
14. Morinaga T, Nakagawa N, Yasuda H, Tsuda E, Higashio K. Cloning and characterization of the gene encoding human osteoprotegerin/osteoclastogenesis-inhibitory factor. Eur J Biochem 254:685–91, 1998 [PubMed: 9688283]
15. Hofbauer LC, Heufelder AE. Role of receptor activator of nuclear factor-kappaB ligand and osteoprotegerin in bone cell biology. J Mol Med 79:243–53, 2001 [PubMed: 11485016]
16. Lories RJ, Luyten FP. Osteoprotegerin and osteoprotegerin-ligand balance: a new paradigm in bone metabolism providing new therapeutic targets. Clin Rheumatol 20:3–9, 2001 [PubMed: 11254237]
17. Lacey DL, Timms E, Tan HL, Kelley MJ, Dunstan CR, Burgess T, Elliott R, Colombero A, Elliott G, Scully S, Hsu H, Sullivan J, Hawkins N, Davy E, Capparelli C, Eli A, Qian YX, Kaufman S, Sarosi I, Shalhoub V, Senaldi G, Guo J, Delaney J, Boyle WJ. Osteoprotegerin ligand is a cytokine that regulates osteoclast differentiation and activation. Cell 93: 165–76, 1998 [PubMed: 9568710]
18. Cundy T, Hegde M, Naot D, Chong B, King A, Wallace R, Mulley J, Love DR, Seidel J, Fawkner M, Banovic T, Callon KE, Grey AB, Reid IR, Middleton-Hardie CA, Cornish J 2002 A mutation in the gene TNFRSF11B encoding osteoprotegerin causes an idiopathic hyperphosphatasia phenotype. Hum Mol Genet 11:2119–2127. [PubMed: 12189164]
19. Mumm S, Banze S, Pettifor J, Tau C, Schmitt K, Ahmed A, et al. Juvenile Paget's disease: molecular analysis of TNFRSF11B encoding osteoprotegerin indicates homozygous deactivating mutations from consanguinity as the predominant etiology (abstract). J Bone Miner Res (Suppl 2): 18:S388, 2003
20. Whyte MP, Singhellakis P, Petersen MB, Davies M, Totty WG, Mumm S. Juvenile Paget's disease: the second reported, oldest patient is homozygous for the TNFRSF11B "Balkan" mutation (966_969deltgacinsctt) which elevates circulating immunoreactive osteoprotegerin levels. J Bone Miner Res 22: 938–46, 2007 [PubMed: 17352649]
21. Saki F, Karamizadeh Z, Nasirabadi S, Mumm S, McAlister WH, Whyte MP: Juvenile Paget's disease in an Iranian kindred with vitamin D deficiency and novel homozygous *TNFRSF11B* mutation. Journal of Bone Mineral Research, 28: 1501–8, 2013 [PubMed: 23322328]
22. Whyte MP, Tau C, McAlister WH, Zhang X, Novack DV, Santini-Araujo E, Preliasco V, Mumm S: Juvenile Paget's disease caused by mutation within *TNFRSF11A* encoding RANK. Bone 68: 153–61, 2014 [PubMed: 25063546]
23. Whyte MP, Kempa LG, McAlister WH, Zhang F, Mumm S, Wenkert D: Elevated serum lactate dehydrogenase isoenzymes and aspartate transaminase distinguish Albers-Schőnberg disease

(chloride channel 7 deficiency osteopetrosis) among the sclerosing bone disorders. Journal of Bone and Mineral Research 25: 2515–26, 2010 [PubMed: 20499337]

24. Eddy MC, Chines A, Silva DP Jr, Landt Y, Ladenson JH: Creatine kinase brain isoenzyme (BB-CK) Presence in serum distinguishes osteopetroses among the sclerosing bone disorders. American Journal of Human Genetics 59: A–349, 1996
25. Whyte MP, Madson KL, Mumm S, McAlister WH, Novack DV, Blair JC, Helliwell TR, Stolina M, Abernethy LJ, Shaw NJ: Rapid skeletal turnover in a radiographic mimic of osteopetrosis. Journal of Bone and Mineral Research 29: 2601–9, 2014 [PubMed: 24919763]
26. Otaify GA, Whyte MP, Gottesman GS, McAlister WH, Gordon JE, Hollander A, Andrews MV, El-Mofty S, Chen W-S, Veis DJ, Stolina M, Woo A, Katsonis P, Lichtarge O, Zhang F, Shinawi M: Gnathodiaphyseal dysplasia: severe atypical presentation from a novel heterozygous mutation in the anoctamin gene (ANO5). Bone 107: 161–71, 2018 [PubMed: 29175271]
27. Mumm S, Gottesman GS, Wenkert D, Campeau PM, Nenninger A, Huskey M, Bijanki VN, Veis DJ, Barnes AM, Marini JC, Stolina M, Zhang F, McAlister WH, Whyte MP. Bruck syndrome 2 variant lacking congenital contractures and involving a novel compound heterozygous PLOD2 mutation. Bone 130: 115047, 2020 [PubMed: 31472299]
28. Kurihara N, Hiruma Y, Yamana K, Michou L, Rousseau C, Morissete J, Galson DL, Teramachi J, Zhou H, Dempster Dw, Windle JJ, Brown JP, Roodman GD. Contributions of the measles virus ncleocapsid gene and the SQSTM1/p62P392L mutation to Paget's disease. Cell Metabolism 13: 23–34, 2011 [PubMed: 21195346]
29. Lapunzina P, Aglan M, Temtamy S, Caparros-Martin JA, Valencia M, Leton R, Martínez-Glez V, Elhossini R, Amr K, Vilaboa N, Ruiz-Perez VL. Identification of a frameshift mutation in Osterix in a patient with recessive osteogenesis imperfecta. American Journal of Human Genetics. 87: 110–4, 2010 [PubMed: 20579626]
30. Adzhubei IA, Schmidt S, Peshkin L, Ramensky VE, Gerasimova A, Bork P, Kondrashov AS, Sunyaev SR. A method and server for predicting damaging missense mutations. Nat Methods. 7: 248–9, 2010. [PubMed: 20354512]
31. Sim NL, Kumar P, Hu J, Henikoff S, Schneider G, Ng PC. SIFT web server: predicting effects of amino acid substitutions on proteins. Nucleic Acids Res. (Web Server issue):W452–7. doi: 10.1093/nar/gks539, 2012. [PubMed: 22689647]
32. The UniProt Consortium. UniProt: a worldwide hub of protein knowledge. Nucleic Acids Res. 47: D506–515, 2019 [PubMed: 30395287]
33. Lu J, Qu S, Yao B, Xu Y, Jin Y, Shi K, Shui Y, Pan S, Chen L, Ma C. Osterix acetylation at K307 and K312 enhances its transcriptional activity and is required for osteoblast differentiation. Oncotarget. 7: 37471–37486, 2016. [PubMed: 27250035]
34. Lui J, Raimann A, Dong L, Hojo H, Roschger P, Fratzl-Zelman N, Jee YH, Haeusler G, Baron J. De novo missense mutation in SP7 in a patient with cranial hyperostosis, long bone fragility, and increased osteoblast number. (Abstract) J Bone Miner Res 34 (Suppl 1): 289, 2019
35. Cole DEC, Whyte MP 1996 Hyperphosphatasia syndromes. In: Cohen MM Jr, Baum BJ (eds.) Studies in Stomatology and Craniofacial Biology. IOS Press, Amsterdam, Netherlands, pp. 245–272.
36. Caffey J Familial hyperphosphatasemia with ateliosis and hypermetabolism of growing membranous bone: review of the clinical, radiographic and chemical features. Bull Hosp Joint Dis 1972;33:81–110. [PubMed: 4648260]
37. Naot D, Wilson LC, Allgrove J, Adviento E, Piec I, Musson DS, Cundy T, Calder AD. Juvenile Paget's disease with compound heterozygous mutations in *TNFRSF11B* presenting with recurrent clavicular fractures and a mild skeletal phenotype. Bone 130: 115098, 2020 [PubMed: 31655221]
38. Kanis JA. Pathophysiology and treatment of Paget's disease of bone. 2nd ed. Malden, Mass.: Blackwell Science, 1998, page 206
39. Singer FR, Roodman GD. Paget's disease of bone. In: Bilezikian JP, Raisz LG, Rodan GA, eds. Principles of bone biology. 2nd ed. San Diego, Calif.: Academic Press, 2001:1249–58.
40. Whyte MP. Paget's disease of bone (clinical practice). N Engl J Med 2006; 355:593–600. [PubMed: 16899779]

41. Scotto di Carlo F, Pazzaglia L, Esposito T, Gianfrancesco F: The loss of Profilin 1 causes early-onset Paget's disease of bone. J Bone Miner Res (in press) 2020.
42. Martin TJ. Paracrine regulation of osteoclast formation and activity: milestones in discovery. J Musculoskelet Nueronal Interact 2004;4:243–53.
43. Boyce BF, Xing L. Functions of RANKL/RANK/OPG in bone modeling and remodeling. Arch Biochem Biophys 2008;473:139–46. [PubMed: 18395508]
44. Bucay N, Sarosi I, Dunstan CR, Morony S, Tarpley J, Capparelli C, Scully S, Tan HL, Xu W, Lacey DL, Boyle WJ, Simonet WS. Osteoprotegerin-deficient mice develop early onset osteoporosis and arterial calcification. Genes Dev 1998; 12:1260–8. [PubMed: 9573043]
45. Hughes AE, Ralston SH, Marken J, et al. Mutations in TNFRSF11A, affecting the signal peptide of RANK, cause familial expansile osteolysis. Nat Genet 2000;24:45–8. [PubMed: 10615125]
46. Sobacchi C, Frattini A, Guerrini MM, Abinun M, Pangrazio A, Susani L, Bredius R, Mancini G, Cant A, Bishop N, Grabowski P, Del Fattore A, Messina C, Errigo G, Coxon FP, Scott DI, Teti A, Rogers MJ, Vezzoni P, Villa A, Helfrich MH. Osteoclast-poor human osteopetrosis because of mutations in the gene encoding RANKL. Nat Genet 2007;39:960–2. [PubMed: 17632511]
47. Guerrini MM, Sobacchi C, Cassani B, Abinun M, Kilic SS, Pangrazio A, Moratto D, Mazzolari E, Clayton-Smith J, Orchard P, Coxon FP, Helfrich MH, Crockett JC, Mellis D, Vellodi A, Tezcan I, Notarangelo LD, Rogers MJ, Vezzoni P, Villa A, Frattini A. Human osteoclast-poor osteopetrosis with hypogammaglobulinemia due to TNFRSF11A (RANK) mutations. Am J Hum Genet 2008; 83:64–76. [PubMed: 18606301]
48. Nakashima K, Zhou X, Kunkel G, Zhang Z, Deng JM, Behringer RR, de Crombrugghe B. "The novel zinc finger-containing transcription factor osterix is required for osteoblast differentiation and bone formation". Cell. 108: 17–29, 2002 [PubMed: 11792318]
49. Renn J, Winkler C Osterix-mCherry transgenic medaka for in vivo imaging of bone formation. Developmental Dynamics 238: 241–8, 2009 [PubMed: 19097055]
50. Hojo H, Ohba S, He X, Lai LP, McMahon AP. Sp7/Osterix is restricted to bone-forming vertebrates where it acts as a Dlx co-factor in osteoblast specification. Developmental Cell 37, 238–253, 2016 [PubMed: 27134141]
51. Renn J, Winkler C. "Osterix-mCherry transgenic medaka for in vivo imaging of bone formation". Developmental dynamics. 238: 241–8, 2009 [PubMed: 19097055]
52. DeLaurier A, Eames BF, Blanco-Sanchez B, Peng G, He X, Swartz ME, Ullmann B, Westerfield M, Kimmel CB. "Zebrafish sp7: EGFP: a transgenic for studyng otic vesicle formation, skeletogenesis, and bone regeneration". Genesis. 48: 505–11, 2010 [PubMed: 20506187]
53. Sinha KM, Zhou X. "Genetic and molecular control of osterix in skeletal formation. Journal of Cellular Biochemistry 114: 975–84, 2013 [PubMed: 23225263]
54. Kaback LA, Soung D, Naik A, Smith N, Schwarz EM, O'Keefe JR, Drissi H. "Osterix/Sp7 regulates mesenchymal stem cell mediated endochondral ossification". Journal of Cellular Physiology. 214: 173–82., 2008 [PubMed: 17579353]
55. Timpson JN, Tobias JH, Richards JB, Soranzo N, Duncan EL, Sims AM, Whittaker P, Kumanduri V, Zhai G, Glaser B, Eisman J, Jones G, Nicholson G, Prince R, Seeman E, Spector TD, Brown MA, Peltonen L, Smith GD, Deloukas P, Evans DM. "Common variants I the region around Osterix are associated with bone mineral density and growth in childhood: Human Molecular Genetics 18: 1510–7, 2009 [PubMed: 19181680]
56. Gilbert L, He X, Farmer P, Boden S, Kozlowski M, Rubin J, Nanes MS. "Inhibition of osteoblast differentiation by tumor necrosis factor-alpha". Endocrinology 141: 3956–64, 2000. [PubMed: 11089525]
57. Tu Q, Valverde P, Li S, Zhang J, Yang P, Chen J. "Osterix overexpression in mesenchymal stem cells stimulates healing of criticalized defects in murine calvarial bone". Tissue Engineering 13: 2431–40, 2007. [PubMed: 17630878]
58. Cao Y, Zhou Z, de Crombrugghe B, Nakashima K, Guan H, Duan X, Jia S-F, Kleinerman ES. "Osterix, a transcription factor for osteoblast differentiation, mediates antitumor activity in murine osteosarcoma". Cancer Research. 65: 1124–8, 2005 [PubMed: 15734992]
59. Taylor JC, Martin HC, Lise S, et al.: Factors influencing success of clinical genome sequencing across a broad spectrum of disorders. Nature Genetics, 47: 7717–26, 2015

Figure 1: Patient age 15 years:

a-c) Hypertelorism with a broad forehead and supraorbital frontal bone prominence is apparent.

Panel **a** is reproduced with permission from *New England Journal of Medicine* Whyte MP, Obrecht SE, Finnegan PM, Jones JL, Podgorink MN, McAlister WH, Mumm S: Osteoprotegerin deficiency and juvenile Paget's disease, 347: 182, 2002.[5]

d-f) The right lower extremity bows anteriorly. Shortening of the left lower extremity underlies pelvic tilt and scoliosis.

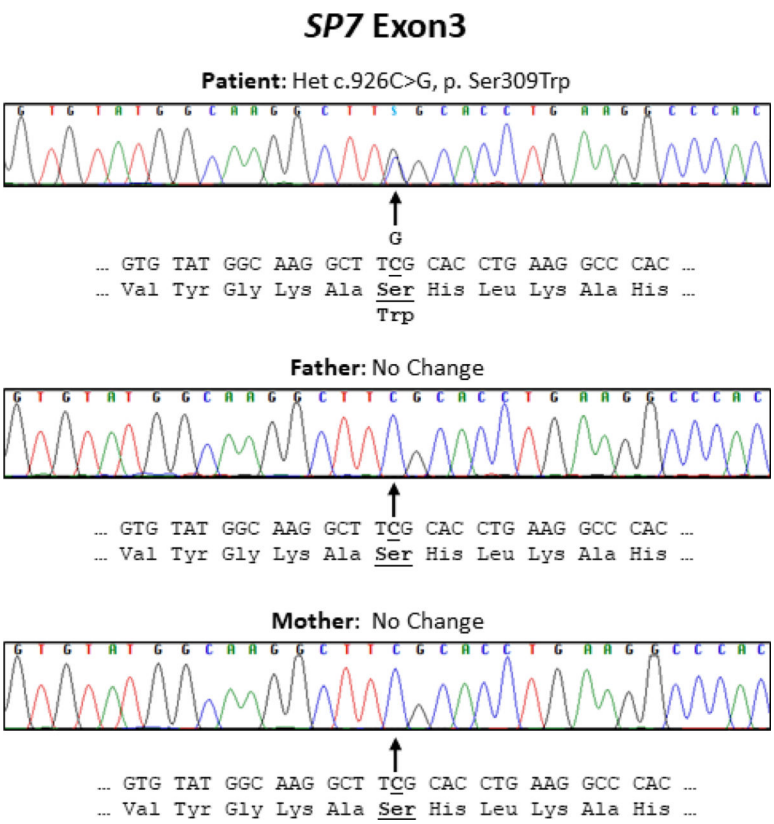

Figure 2: Patient's de novo *SP7* mutation

Our patient's and her parents' electro-pherograms highlight her sporadic heterozygous missense variant in *SP7* exon 3 that is absent in her parents. The cDNA and amino acids sequences are shown in bold as well as underlined to indicate the altered base and amino acid, respectively.

Figure 3: Referral Skeletal Radiographic Findings

a) At age 2 years, anteroposterior (AP) and lateral view of the right tibia and fibula have considerable processing artifact. Note, however, the AP bowing with osteosclerosis (trabecular thickening) and hyperostosis (cortical thickening).

b) At age 3 years, a transverse “chalk stick” pathologic fracture involves the right femur through diffusely dense bone.

c) At an older age, the right distal femur has fractured similarly.

d) AP view of the laterally bowed right femur shows striking osteosclerosis and hyperostosis with obliteration of the medullary space proximally.

e) AP view of the right tibia/fibula also shows marked osteosclerosis and hyperostosis with constriction of the medullary cavity and proximally a transverse fracture (arrowhead). Osteosclerotic striations are apparent in the distal metaphysis. The mid-portion of the fibula has been removed.

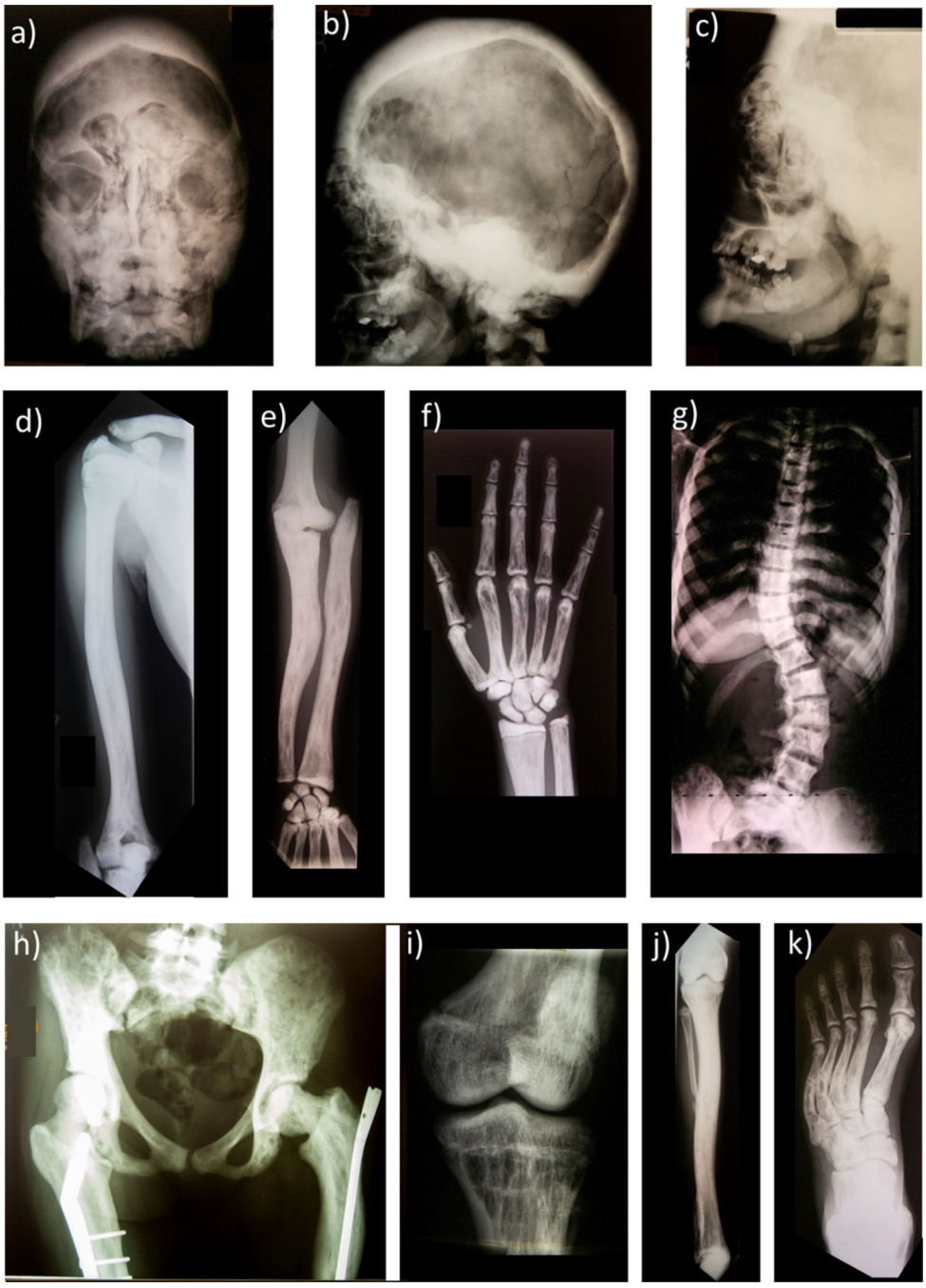

Figure 4: Radiographic Skeletal Survey At Age 15 Years:

a) Skull anteroposterior (AP) and **b)** lateral view [reproduced with permission from *New England Journal of Medicine* Whyte MP, Obrecht SE, Finnegan PM, Jones JL, Podgorink MN, McAlister WH, Mumm S, Osteoprotegerin Deficiency and Juvenile Paget's Disease,[5] 347: 182, 2002. Copyright © (2002) Massachusetts Medical Society] and **c)** lateral face show profound thickening of a markedly sclerotic diploic space containing small lucencies throughout. The skull base and maxilla and petrous bones are markedly osteosclerotic. Sinuses have developed, but the frontal sinuses contain osteosclerotic filling defects. Marked

hypertelorism is present. The mandible is diffusely osteosclerotic with cortical thickening. The teeth are markedly deformed with hypoplastic roots (Figure 6).

d) Right AP humerus shows osteosclerosis with marked cortical thickening encroaching on the medullary cavity that is largely obliterated proximally. Linear lucencies and coarse trabeculae affect the distal humerus.

e) Right forearm shows radial head dislocation and deformity lacking articulation with the humerus. Bowing deformities of both forearm bones accompanies diffuse osteosclerosis, obliteration of the medullary cavities, and linear and small lucencies scatted throughout.

f) Right hand demonstrates some lack of modeling in the distal radius and ulna, diffuse osteosclerosis, and marked coarse linearly thick trabeculae. Patchy sclerosis affects the middle and distal phalanges. The carpal bones are almost uniformly sclerotic with small lucencies.

g) AP chest and thoracic and lumbar spine demonstrate diffusely and markedly sclerotic vertebrae with scoliosis. The lumbar vertebrae have an “hourglass” indentation anteriorly. The ribs are markedly sclerotic and expanded with small longitudinal lucencies with thick trabeculae throughout.

h) AP pelvis shows asymmetry, diffuse marked sclerosis with varying-sized small lucencies including linear ones, and distorted thick trabeculae. Coxa valga is present on the right, with a femoral plate and screws. Coxa vara on the left accompanies an intramedullary rod.

i) AP of right leg demonstrates marked osteosclerosis, cortical thickening with loss of the medullary cavity, coarse linear striations of bones primarily in the metaphyses, bowing the of the right tibia, and partial absence of the mid-right fibula (presumably from surgical resection).

j) AP left knee scanogram shows sclerotic coarse trabeculae.

k) AP left foot shows heel and forefoot varus with overall osteosclerosis, prominent linear longitudinal lucencies, and linear coarse striata-appearing trabeculae. Incomplete fractures of the metatarsals are present bilaterally.

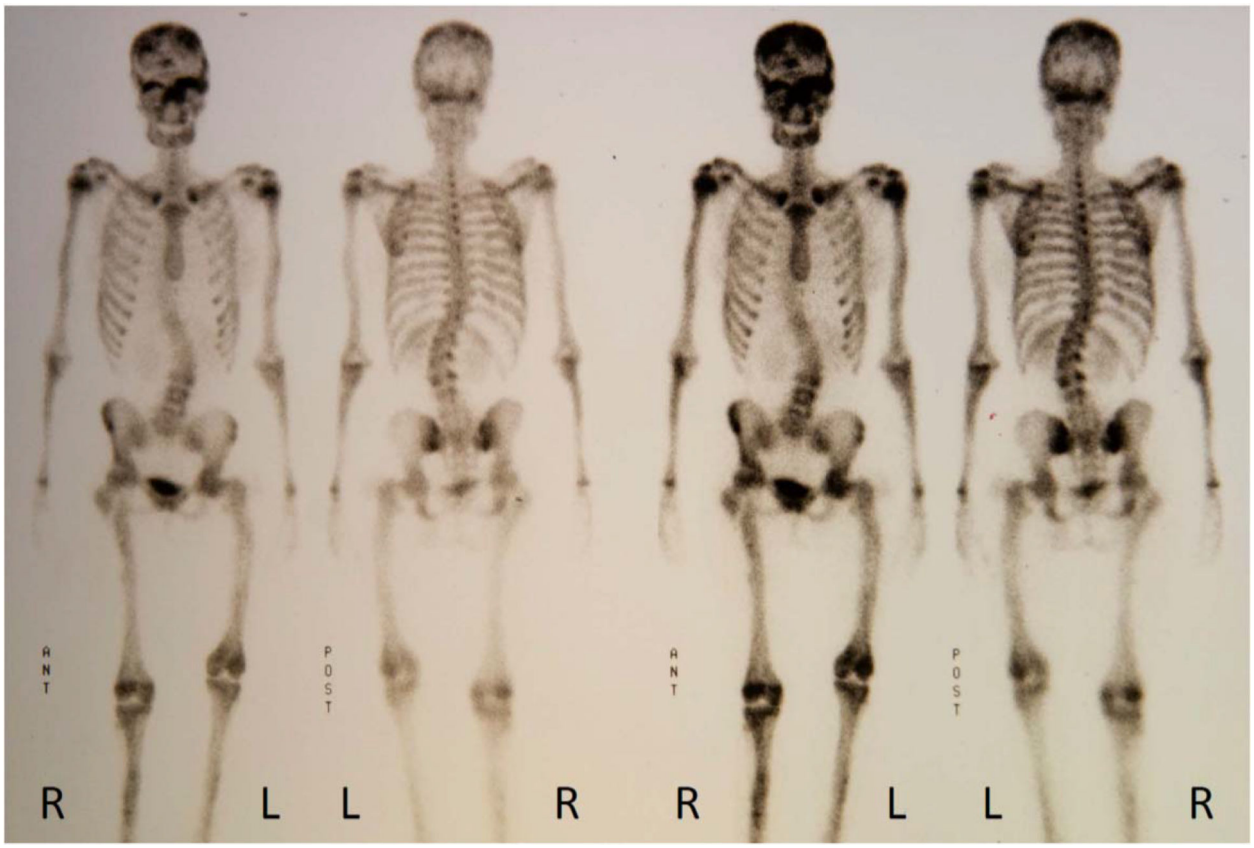

Figure 5: Skeletal Scintigraphy At Age 15 Years

Foci of increased activity are apparent in the parietal region of the skull bilaterally. A focus of intense activity involves the supraorbital region (left greater than the right) and extends centrally either involving the ethmoid plate or adjacent sphenoid. Symmetric, moderately increased activity involves both proximal humeri, likely corresponding to the physeal plates given its symmetry. Deformity of the long bones of the lower extremities (not illustrated distally) involves most prominently both proximal femurs both with evidence of internal fixation hardware. The left lower extremity is shorter than the right, particularly the femoral component. Moderate levoscoliosis curves the lumbar spine. Intensely increased activity is focused in the anterior distal metaphyseal region of the right femur. Focal increased activity in the anterior right proximal tibial metaphysis is non-specific, perhaps representing a healing fracture.

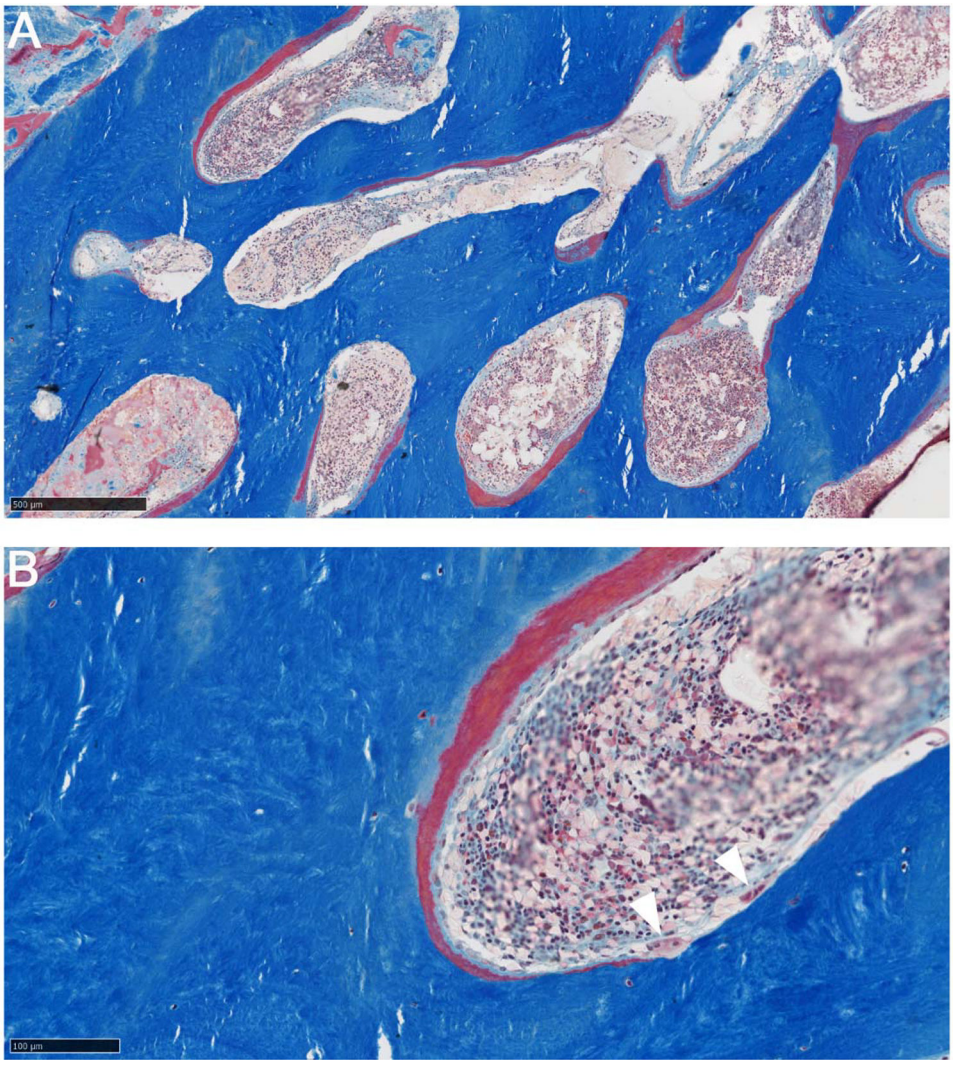

Figure 6: Iliac Crest Histopathology

Masson trichrome stain (A,B) does not show clear evidence of woven bone, as there is no increase in the number or size of osteocytes or an abnormal distribution. Thick layers of osteoid are present, covered by osteoblasts. Osteoclasts, of normal morphology, are also present (white arrowheads). Regardless of presence or absence of woven bone, the appearance is of high bone turnover.

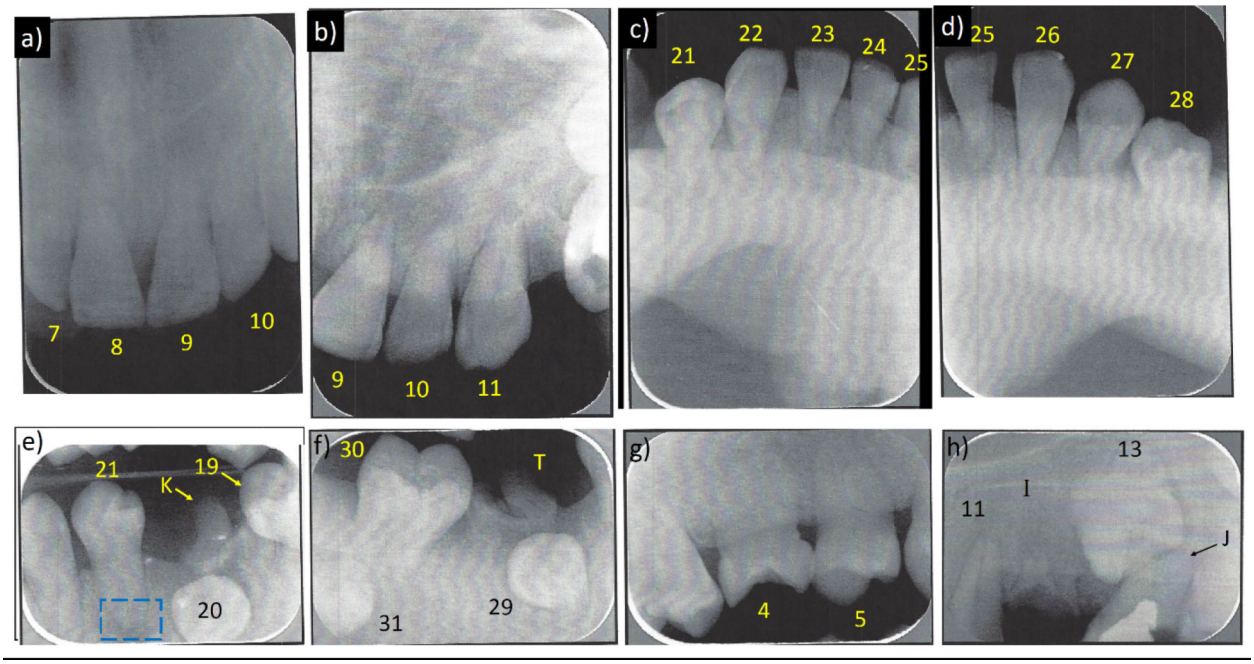

Figure 7: Patient's Dental Radiography At Age 15 Years

a) Teeth #7–10 and **b)** #9–11 have no (or a very thin) pulp canals, only 1/3 of their roots formed, and blunt apices.

c) Very thin pulp canals are present in teeth #21–25 and **d)** #25–28, only 1/3 of roots are formed, and the root apices are blunt. There are enlarged periodontal ligaments.

e) Tooth #19 and primary tooth #K require extraction. Tooth #20 is bony impacted and requires extraction. Teeth #21 and #22 have very thin (or no) pulp canals, no pulp chamber, only 1/3 of roots formed, and blunt apices. Some radiolucency at the apex of tooth #21 (blue box) could reflect a closed apex with an enlarged periodontal ligament.

f) Primary tooth #T is badly broken and requiress extraction. Teeth #29 and #31 are bony impacted and require extraction. Tooth #30 has very small pulp canal with no pulp chamber, only 1/3 of its root formed, and a blunt apex.

g) Tooth #4 is rotated 90°, tooth #5 is rotated 45°, and tooth #6 has a very small or no pulp chamber. The roots are 1/3 formed with blunt apices.

h) Primary tooth #J has been treated by pulpotomy, but needs extraction. Tooth #13 is bony impacted and needs extraction. Tooth #11 has a very thin pulp canal with enlarged periodontal ligament. Root tips of tooth #I are present.

Table 1

Biochemical Findings

Test	Units	Patient	Adult Reference Range
Serum			
Calcium	mg/dl	9.4	8.8 – 10.6
Ionized Ca^{++}	″	4.9	4.5 – 5.3
Phosphorus (Pi)	″	5.0, 4.8	2.9 – 5.4
25(OH)D [+]	ng/ml	14	13 – 67
$1,25(OH)_2D$ [+]	pg/ml	61	27 – 71
PTH	″	91	10 – 65
Alkaline phosphatase	U/L	1178	130 – 550
Urea	mg/dl	9	7 – 18
Creatinine	″	0.5	0.5 – 1.4
Total protein	g/dl	6.5	6.0 – 8.5
Albumin	″	3.3	3.4 – 5.2
Uric acid	mg/dl	5.5	2 – 6.5 ♀
Magnesium	″	1.7	1.6 – 2.2
Sodium	mmol/L	138	136 – 145
Potassium	″	3.8	3.6 – 5.3
Chloride	″	106	96 – 106
Bicarbonate	″	24	22 – 31
Glucose	mg/dl	76	65 – 109
AST	U/L	20	10 – 45
Acid phosphatase [+]	″	4.3	2.3 – 5.0
LDH	″	416	300 – 750
Bilirubin	mg/dl	2.1	0.2 – 1.2
IGF1 [+]	ng/ml	243	261 – 1096
Creatine kinase	IU/L	73	26 –170
Hemogram			
Hemoglobin	g/dl	10.9	12 – 16
White blood cells	$x10^3$/ul	3.1	4.8 – 10.8
Platelets	$Kx10^3$/ul	156	150 – 450
Prothrobin time	seconds	14.2	11.2 – 13.2
Partial thromboplastin time	seconds	25.1	21 – 31.8
Urine[‡]			
Creatinine Clearance	mls/min	166, 143	79 – 187
Osmolality	mOSM	660	50 – 1200
Calcium/Creatinine	mg/g crt	< 20, < 26	< 250

Test	Units	Patient	Adult Reference Range
Deoxypyridinoline [+]	nmol/mmol crt	22.7	≤ 59
Hydroxyproline [+]	mg/g crt	233	7 – 49
Free Hydroxyproline [+]	mg/g crt	1.4	< 2.7
Tubular reabsorption Pi (TRP)	%	94, 94	78 – 91
TmP/GFR	mg/dl	4.7, 4.5	2.5 – 4.2

[+]Quest Diagnostics Inc.; San Juan Capistrano, CA, USA

[≠]Routine urinalysis normal